

# Estimating net radiation at surface using artificial neural networks: a new approach

Antonio Geraldo Ferreira · Emilio Soria-Olivas ·  
Antonio José Serrano López · Ernesto Lopez-Baeza

Received: 11 March 2010 / Accepted: 7 July 2011 / Published online: 19 July 2011  
© Springer-Verlag 2011

**Abstract** This study describes the results of artificial neural network (ANN) models to estimate net radiation ( $R_n$ ), at surface. Three ANN models were developed based on meteorological data such as wind velocity and direction, surface and air temperature, relative humidity, and soil moisture and temperature. A comparison has been made between the  $R_n$  estimates provided by the neural models and two linear models (LM) that need solar incoming shortwave radiation measurements as input parameter. Both ANN and LM results were tested against in situ measured  $R_n$ . For the LM ones, the estimations showed a root mean square error (RMSE) between 34.10 and 39.48  $\text{Wm}^{-2}$  and correlation coefficient ( $R^2$ ) between 0.96 and 0.97 considering both the developing and the testing phases of calculations. The estimates obtained by the ANN models showed RMSEs between 6.54 and 48.75  $\text{Wm}^{-2}$  and  $R^2$  between 0.92 and 0.98 considering both the training and the testing phases. The ANN estimates are shown to be similar or even better, in some cases, than those given by the LMs. According to the

authors' knowledge, the use of ANNs to estimate  $R_n$  has not been discussed earlier, and based on the results obtained, it represents a formidable potential tool for  $R_n$  prediction using commonly measured meteorological parameters.

## 1 Introduction

Net radiation is the most significant energy exchange quantity on Earth because it represents the limit to the available energy source or sink for physical and biophysical processes, thus constituting the fundamental parameter governing the lower atmosphere climate (Oke 1987; Iziomon et al. 2000). The surface net radiative energy balance can be calculated by using:

$$R_n = R_s^\downarrow - R_s^\uparrow + R_1^\downarrow - R_1^\uparrow. \quad (1)$$

This equation represents the algebraic sum of both shortwave  $R_s$  and longwave  $R_1$  radiation flux densities, where the downward ( $\downarrow$ ) and upward ( $\uparrow$ ) arrows, respectively, indicate incoming and outgoing radiation components at the surface (Fig. 1). According to the arrows in Eq. 1, the downward incident radiation is taken as positive, while the upward emerging radiation is taken as negative.

The outgoing shortwave  $R_s^\uparrow$  is the fraction of the shortwave incoming solar radiation  $R_s^\downarrow$  that is reflected by the surface under consideration, i.e.,

$$R_s^\uparrow = \alpha R_s^\downarrow, \quad (2)$$

where  $\alpha$  is the surface albedo. Thus, Eq. 1 can be rewritten as

$$R_n = (1 - \alpha)R_s^\downarrow + (R_1^\downarrow - R_1^\uparrow). \quad (3)$$

---

A. G. Ferreira · E. Lopez-Baeza  
Department of Physics of the Earth and Thermodynamics,  
Faculty of Physics, University of Valencia,  
Calle Dr Moliner 50,  
46100 Burjassot, Valencia, Spain

E. Soria-Olivas · A. J. S. López  
Department of Electronic Engineering, ETSE,  
University of Valencia,  
Calle Dr Moliner 50,  
46100 Burjassot, Valencia, Spain

A. G. Ferreira (✉)  
Fundação Cearense de Meteorologia  
e Recursos Hídricos—FUNCEME,  
Av. Rui Barbosa,  
1246—CEP 60115-221 Fortaleza, Ceará, Brazil  
e-mail: antonio.ferreira@uv.es

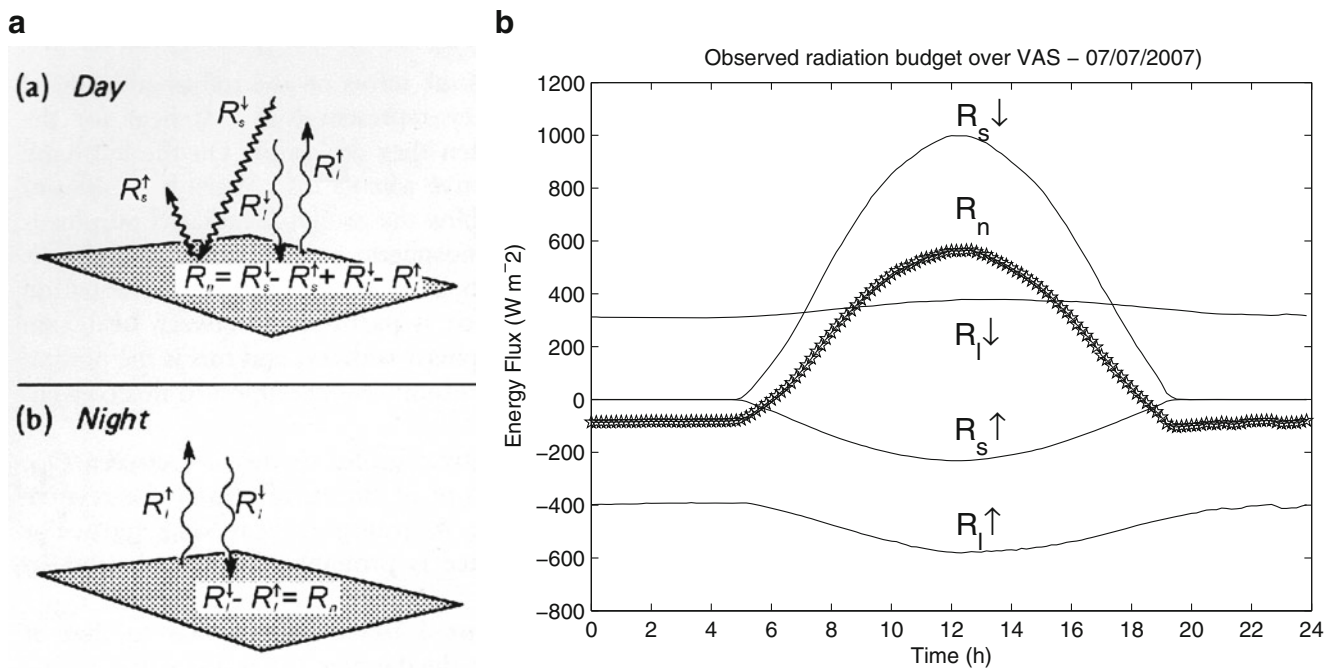


**Fig. 1** a Schematic summary of the fluxes involved in the radiation budget of an “ideal” site, b observed radiation budget over the *Valencia Anchor Station* (latitude  $39^\circ34'15''$  N and longitude  $1^\circ17'18''$  W at the Utiel-Requena Plateau, Spain) under clear sky conditions on July 7, 2007

For natural surfaces, the emission of longwave radiative flux is given by the modified Stefan–Boltzmann law, assuming a given emissivity for the Earth’s surface (Arya 1988). Then, the net radiation flux at the surface is given by

$$R_n = (1 - \alpha)R_s^\downarrow + (R_i^\downarrow - \varepsilon\sigma T_{\text{sfc}}^4), \quad (4)$$

where  $\varepsilon$  is the surface emissivity,  $T_{\text{sfc}}$  the surface temperature (K), and  $\sigma$  the Stefan–Boltzmann constant ( $\sigma = 5.670 \times 10^{-8} \text{ W m}^{-2} \text{ K}^{-4}$ ). Equation 4 shows that the net radiative flux is the result of the radiation balance at the surface and is influenced by the climate near the ground and other properties such as surface temperature, albedo, and emissivity. Since its magnitude is directly related to the various radiative fluxes reaching or outgoing from the surface, it is clear that  $R_n$  is a key parameter for surface energy budget studies.

Despite its importance,  $R_n$  is measured routinely, with net radiometers, only at very few climatological stations around the world, or by scientists in short-term studies, partly because of the problem of providing a standard surface, but also because net radiation instruments are cumbersome to maintain (Irmak et al. 2003; Monteith and Unsworth 1990). As a consequence, a number of studies have put major effort into the accurate determination of  $R_n$  for a given location, considering its land cover and land use, from meteorological data, like soil surface and air temperature, fraction of the sky covered by clouds, relative

humidity, radiation emitted by the atmosphere, and incoming solar radiation, giving origin to various models that have been proposed or evaluated by Carrasco and Ortega-Farías (2007), de Jong et al. (1980), Irmak et al. (2003), Jegede et al. (2006), Kjaersgaard et al. (2007), Wang and Liang (2008), etc. These models based on empirical equations and coefficients either from the literature or based on the physical principles of radiation balance differ from each other in terms of the complexity of the required meteorological data (Sentelhas and Gillespie 2008). However, looking more carefully, most of the  $R_n$  equations utilized to estimate hourly, daily, or long-term  $R_n$  values need incoming solar radiation as input parameter—not a currently measured parameter in the majority of meteorological stations. Taking this into account, the objectives of the present study are (1) the development of a new model for estimating  $R_n$  over a vine crop employing artificial neural networks (ANNs) from routinely observed meteorological data, (2) the application of the two most commonly considered  $R_n$  linear estimation models using incoming solar radiation and albedo as input parameters, and (3) the analysis and comparison of the performance of the LMs against the new proposed ANN model.

The estimated  $R_n$  values from both LM and ANN models were compared to in situ  $R_n$  values measured during a field campaign denominated FESEBAV-2007 (*Field Experiment on Surface Energy Balance Aspects over the Valencia Anchor Station area*) carried out between June 19th and September 18th 2007. The Valencia Anchor Station is a

**Table 1** Description and arrangement of the sensors used for the measurements of the different meteorological and soil parameters during the FESEBAV-07 field campaign

Parameter	Instrument	Manufacturer	Elevation
Net radiation	CN1 Net Pyrradiometer	Middleton & Co. Pty. Ltd.	2 m
Incident and reflected solar radiation	Albedometer CM-14	Kipp and Zonen	2 m
Soil heat flux	RIMCO HP3 Heat Flux Plate	Middleton & Co. Pty. Ltd.	-7.5 cm; -12.5 cm
Air temperature	PT 100/3	Campbell Scientific Ltd.	2 m
Soil temperature	PT 100/3	Campbell Scientific Ltd.	Surface; -5 cm; -10 cm; -15 cm; -25 cm
Relative humidity	HMP45C	Campbell Scientific Ltd.	2 m
Wind speed/direction	RM Young 05103	R. M. Young Company	2.10 m
Soil moisture content	ThetaProbe Soil Moisture Sensor-ML2x	Delta-T Devices Ltd.	-5 cm; -35 cm horizontally

reference meteorological station (39°34'15" N, 1°17'18" W, elevation 813 m above sea level) that was mainly set up for the validation of low spatial resolution satellite data and products.

**2 Material and methods**

**2.1 Description of the experimental site**

In order to better achieve the objective of this study and considering that several meteorological factors as well as land cover and land use do affect the quantity of  $R_n$  that is registered at any particular place, an automatic agrometeorological station was mounted inside a vineyard (39°31'23" N, 1°17'22" W, elevation 796 m above sea level), during the FESEBAV-2007 field campaign mentioned earlier.

The area where FESEBAV-2007 took place is located over the natural region of Utiel-Requena Plateau, Spain. It represents a reasonably homogeneous area of about 50 km×50 km (NW -1.5734, 39.8045; NE -0.9897, 39.7958; SE -1.0026, 39.3455; SW -1.5826, 39.3541) primarily dedicated to vineyard crops. The wines represent about 70–80% of the vegetation cover in the region. The land use of the remaining area is primarily dedicated to dryland crops, almonds, and olives trees, and to a lesser extent, pines and scrubs are also found. The climate in this area is a typical Mediterranean semiarid climate with an average monthly temperature varying between 5.6°C and 7.0°C in winter and between 21.2°C and 25°C in summer. The total annual rainfall is about 461 mm and the average monthly rainfall in the region is between 12 and 61 mm, mainly falling during the autumn months, but spread evenly throughout the year except in the summer dry period between July (12 mm) and August (21 mm).

The area observed by the agrometeorological station corresponds to an extensive plantation of vines distributed in northwest to southeast rows 2.9 m apart with 2.1 m between stumps. The grapevines belong to the typical Spanish *tempranillo* variety and were trained in vertical trellis with the main wire about 1 m above the soil surface. The soil is sandy loam and the laboratory analysis gave a composition of 67% sand, 13% silt, and 20% clay, with bulk density of 0.77 gcm<sup>-3</sup>, 70.9% porosity, and volumetric heat capacity varying between 1.57×10<sup>6</sup> and 1.87×10<sup>6</sup> J m<sup>-2</sup> K<sup>-1</sup>, depending on soil moisture content, that at a depth of 5 cm, ranged between 0.066 and 0.290 m<sup>3</sup> m<sup>-3</sup>, along FESEBAV-2007. During the 92 days of the field campaign, mainly covering the summer season and the full vineyard phenological cycle, nine rainfall events were registered, with three of them presenting a significant daily total rainfall of 35 mm (day 48, August 5, 2007), 20 mm (day 49, August 6, 2007), and 51 mm (day 69, August 26, 2007). In the other 6 days, the daily total rainfall varied between 1 and 7 mm.

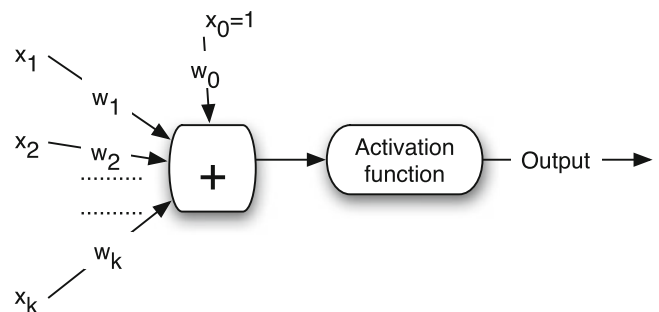
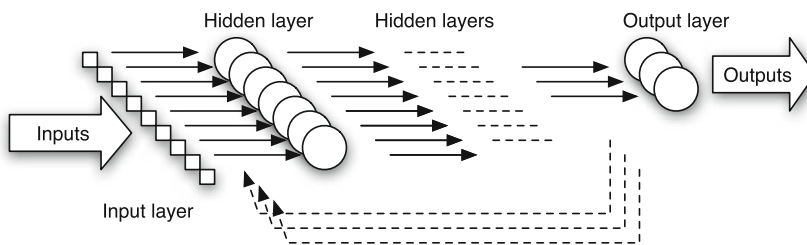


**Fig. 2** Scheme of a neuron;  $x_i$  are the inputs and  $w_j$  are the neuron weights

**Fig. 3** Scheme of a multilayer perceptron



2.2 Instrumentation and measurements

The agrometeorological station installed within the vine field was operated continuously for almost 4 months,

during the 2007 vine growing season, collecting the following parameters: air temperature (degree Celsius), relative humidity (percent), wind direction (degrees), and speed (meter per second); surface temperature and soil

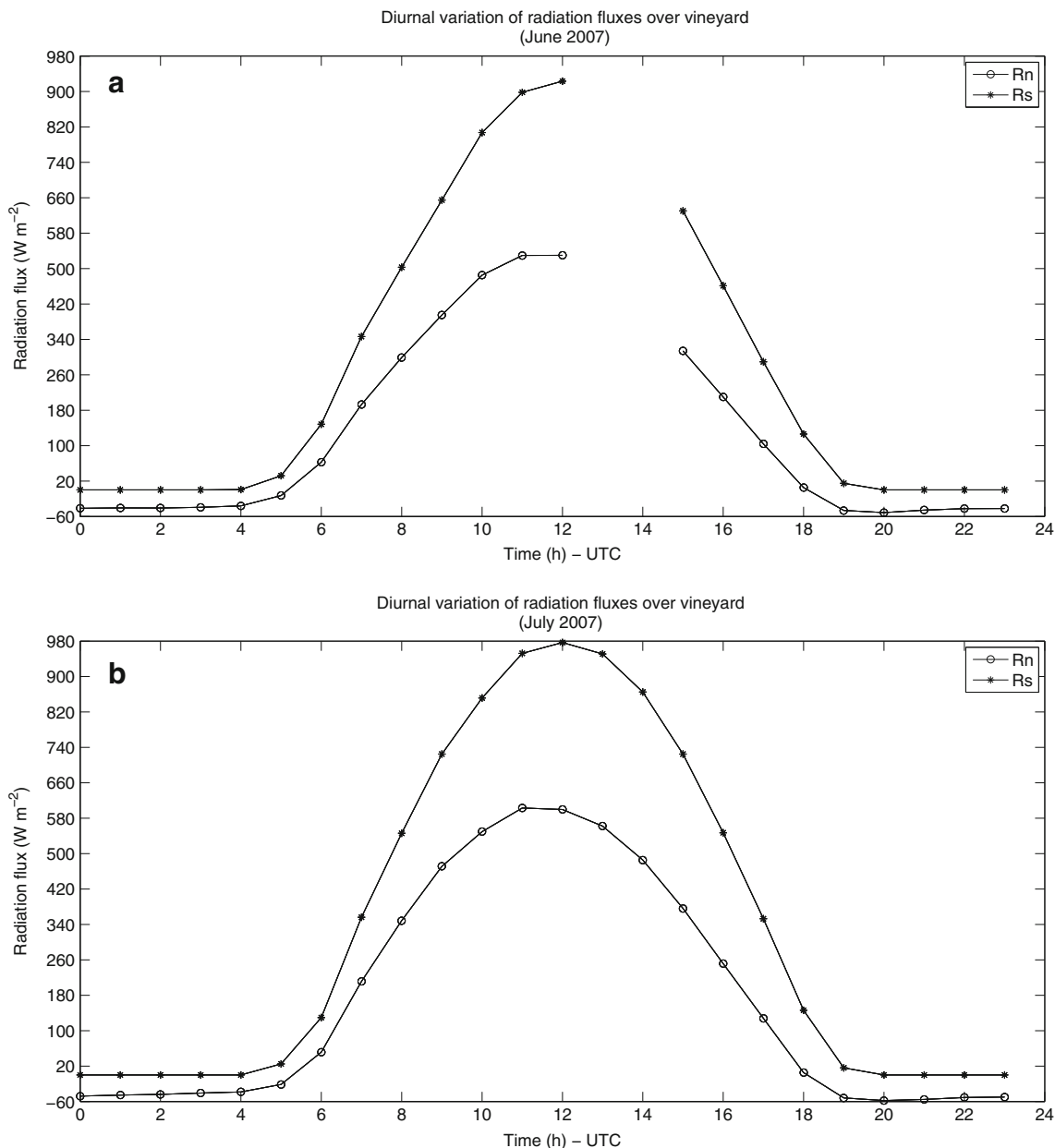


**Fig. 4** Average diurnal variation of measured net radiation ( $R_n$ ) and incoming shortwave radiation ( $R_s$ ) over a vineyard in the period June 19 to September 18, 2007. **a** June 2007, **b** July 2007, **c** August 2007, and **d** September 2007

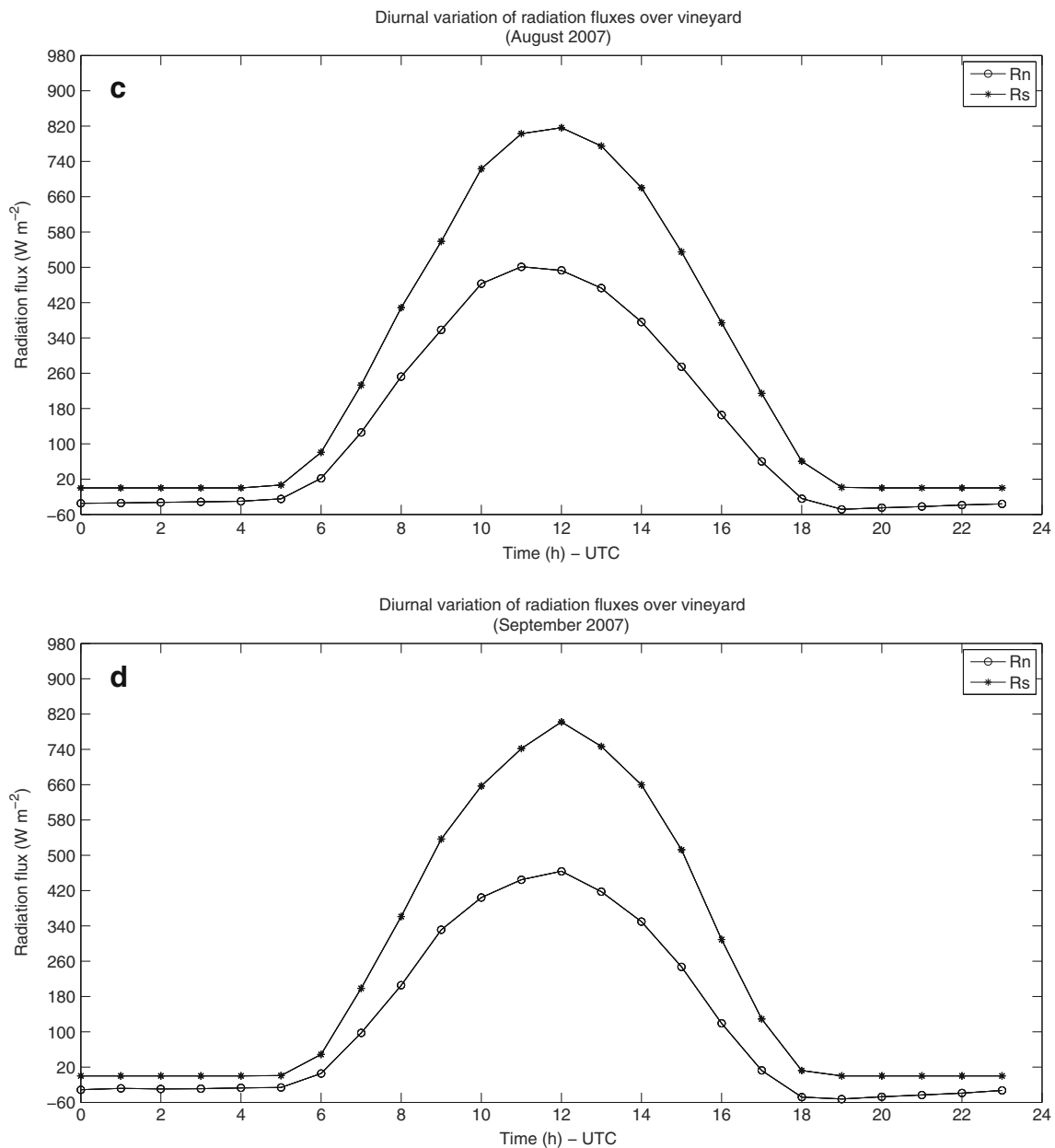


Fig. 4 (continued)

temperature profile (degree Celsius); soil heat flux (watt per square meter); incident, reflected, and net radiation (watt per square meter); and soil moisture (cubic meter per cubic meter). The different sensors (Table 1) were integrated into

**Table 2** Linear regression models obtained for  $R_n$  and statistical results of the comparison between observed and estimated values of  $R_n$

Model	$R^2$	RMSE	MAE	ME	$N$
$R_{n1} = a_1 R_s^1 + b_1$					
$R_{n1} = 0.657 R_s^1 - 54.273$	0.96/0.97	39.48/35.38	34.19/30.87	0.006/7.10	4,397/2,198
$R_{n2} = a_2(1 - \alpha)R_s^1 + b_2$					
$R_{n2} = 0.791(1 - \alpha)R_s^1 - 54.161$	0.96/0.97	37.85/34.10	32.94/30.15	-0.0097/8.21	4,397/2,198

$R^2$ , RMSE, MAE, ME, and  $N$  (number of data utilized). The results are given both for the developing and the testing phases, respectively, separated by /. RMSE, MAE, and ME are in units of watt per square meter

two Campbell CR1000 dataloggers that were programmed to collect the data every second for all sensors and average it for 10 min.

### 2.3 Methods

Since  $R_n$  can be positive, negative, or even zero, in order to better investigate its behavior during the field campaign, the dataset was divided in three parts: The first one considers all  $R_n$  in situ measured data, the second one considers only the negative net radiation ( $R_n < 0$ ) values, and the third one

considers only the positive net radiation ( $R_n > 0$ ) values, hereafter referred to as  $R_{n\pm}$ ,  $R_{n-}$ , and  $R_{n+}$ , respectively. This procedure allows to find a model for  $R_{n\pm}$  overall values and more specific models for  $R_{n-}$  and  $R_{n+}$ . Besides this, each of these datasets was divided into two subsets: the first one comprising two thirds of the data and was used to develop the LM and to train the ANN, and the remaining one third of the data were used for testing the models. The accuracy of the  $R_n$  estimated values using both the LM and the ANN models was assessed through the mean value of the absolute error (MAE), the mean error (ME),  $R^2$ , and root mean square error (RMSE).

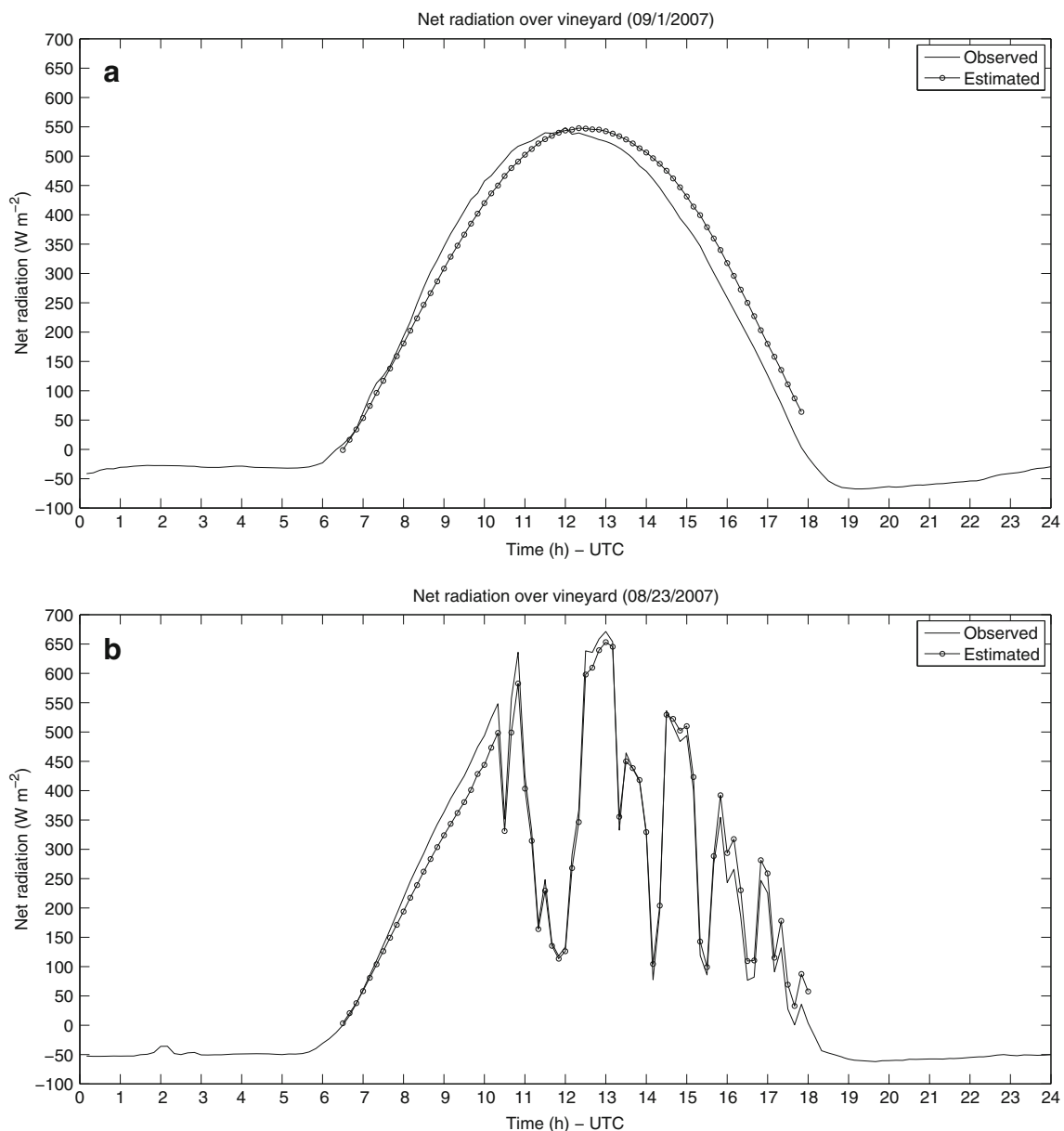


**Fig. 5** Observed and estimated  $R_n$  for cloudless conditions (days: September 1, 2007 and August 15, 2007) and cloudy conditions (days: August 23, 2007 and July 12, 2007). The linear models utilized to

estimate  $R_n$  were:  $R_{n1} = 0.657 R_s^l - 54.273$  for **a** and **b**, and  $R_{n2} = 0.791(1 - \alpha) R_s^l - 54.161$  for **c** and **d**

### 2.3.1 Linear models

Models for calculating  $R_n$  from other climatic parameters using regressions are widely used, including linear regression models, which are formal means of expressing the relationship between two or more variables, and have the power to empirically facilitate complicated relationships among the considered quantities. According to Kjaersgaard et al. (2007), the most commonly used equations to estimate  $R_n$  are

$$R_n = a_1 R_s^\downarrow + b_1 \tag{5}$$

$$R_n = a_2(1 - \alpha)R_s^\downarrow + b_2, \tag{6}$$

where  $a_1$ ,  $a_2$ ,  $b_1$ , and  $b_2$  are regression coefficients,  $\alpha$  represents the surface albedo, and  $R_s^\downarrow$  is the incoming solar radiation that is more commonly measured than  $R_n$ . The investigations have shown that the regression coefficients in those models are, among other things, dependent on the type of surface and its conditions.

### 2.3.2 Multilayer perceptron

Artificial neural networks are mathematical models that learn and establish nonlinear relationships between two datasets. They have the ability to find complex relationships in data (Bishop 1996; Haykin 1999). In this work, the ANN used is the *multilayer perceptron* (MLP), a model that

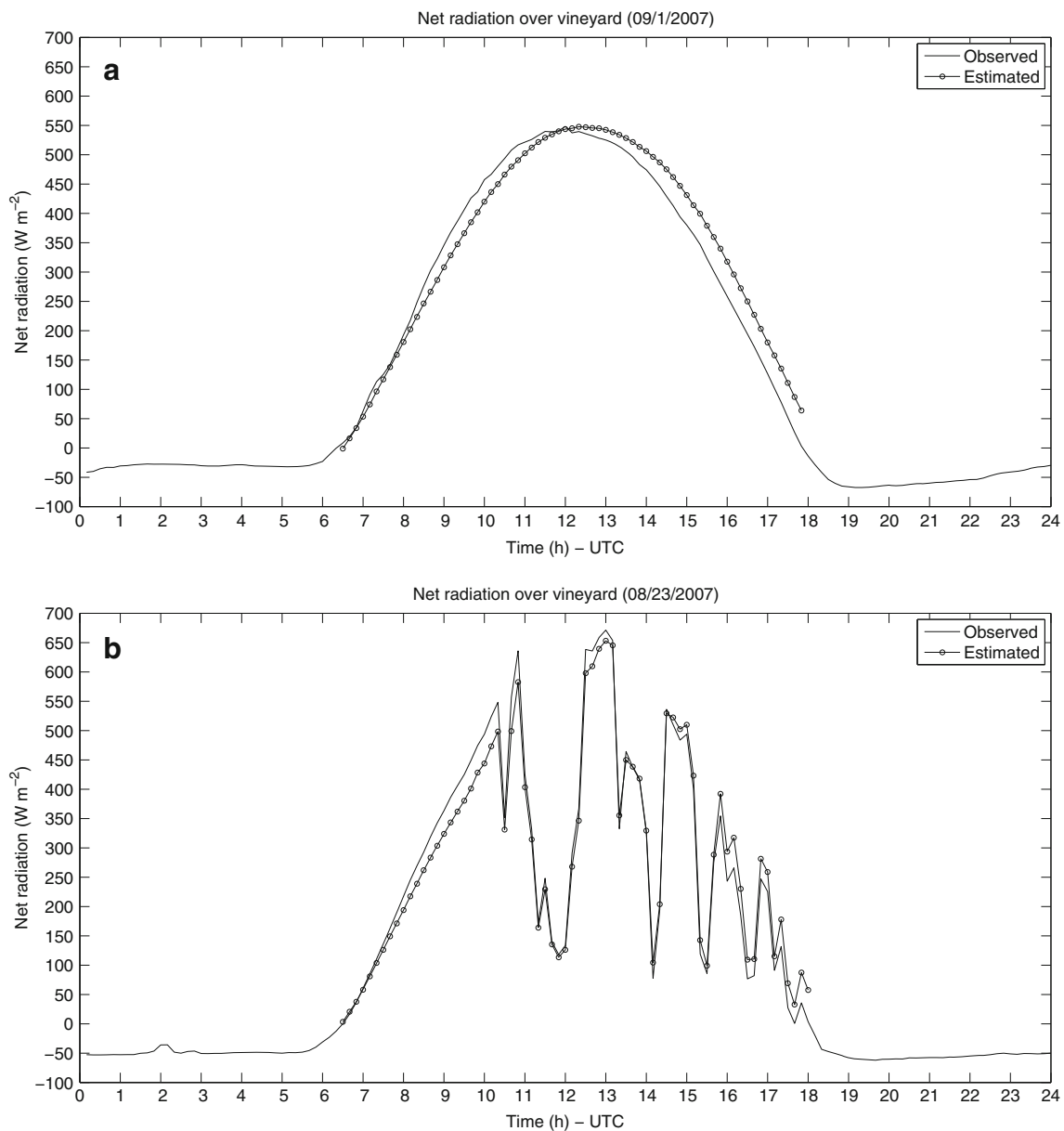


Fig. 5 (continued)



consists in a layered arrangement of individual computation units known as *artificial neurons*. The neurons of a given layer feed with their outputs the neurons of the next layer. A single neuron is shown in Fig. 2.

The inputs  $x_i$  to a neuron are multiplied by adaptive coefficients  $w_i$ , called *synaptic weights* which represent the connectivity between neurons. The output of a neuron is

usually taken to be a sigmoid-shaped (sigmoid or hyperbolic tangent function)  $\varphi$ . The output of the  $j$ th neuron is given by

$$O_j = \varphi \left( \sum_{i=0}^m w_{ij} x_i \right), \quad (7)$$

where  $\varphi$  is a nonlinear function named *activation function*.

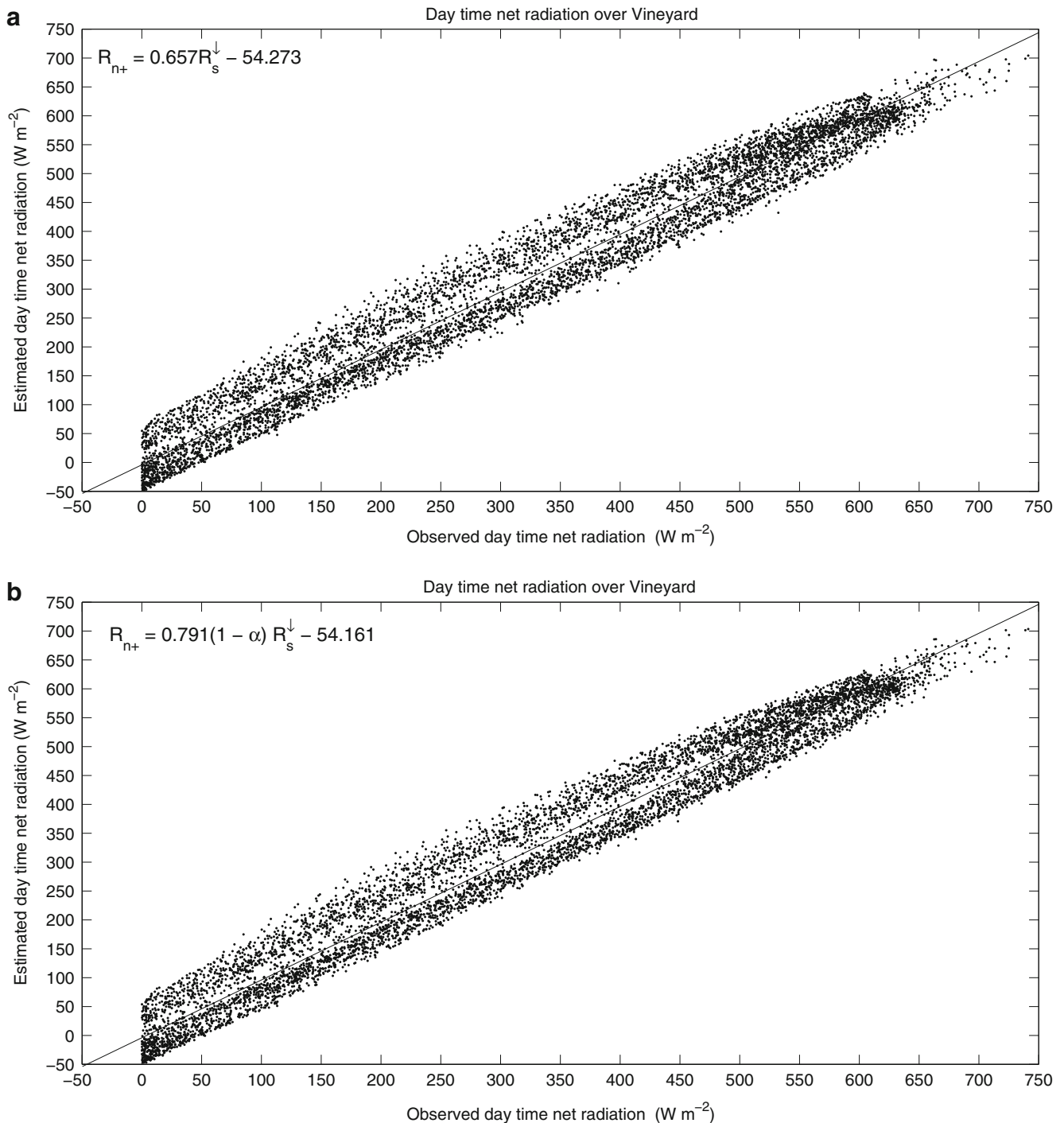


**Fig. 6** Scatter plots of net radiation (observed versus estimated values) for both  $R_{n1}$  (**a**) and  $R_{n2}$  (**b**) models for daytime



**Table 3** Statistical values of the 10-min meteorological parameters utilized as input parameters in the ANN models for the training and validation set

Meteorological parameters	Statistics			
	Min	Max	Mean	Std
Wind velocity (m s <sup>-1</sup> )	0.0	5.05	1.22	0.73
Wind direction (deg)	0.0	359.90	158.98	92.81
Air temperature (°C)	8.81	39.92	21.83	6.45
Surface temperature (°C)	10.63	61.91	28.85	13.12
Soil temperature at 5 cm depth (°C)	14.16	41.70	25.84	6.12
Relative humidity (%)	6.89	99.30	54.74	25.87
Soil moisture at 5 cm depth (m <sup>3</sup> m <sup>-3</sup> )	0.07	0.29	0.09	0.03
Soil heat flux at depth of 7.5 cm (W m <sup>-2</sup> )	-22.54	50.68	-8.49	18.46
Net radiation <sup>a</sup> (W m <sup>-2</sup> )	-73.33	741.30	144.94	231.24

*Min* minimum, *Max* maximum, *Std* standard deviation

<sup>a</sup>Net radiation was considered as output parameter in the ANN models

Neurons from a specific network are grouped together in layers that form a fully connected network. The first layer contains the input nodes, which are usually fully connected to hidden neurons, and these are, in turn, connected to the output layer. Figure 3 shows a scheme of a fully connected multilayer perceptron. In our case, only one output neuron is necessary, since only one parameter is predicted at each time.

### 3 Results and discussion

The diurnal courses of  $R_n$  and  $R_s^\downarrow$  observed during FESEBAV-2007 are presented in Fig. 4. It can be seen that the maximum values of these parameters are reached around midday (UTC), and July is the month in which  $R_s^\downarrow$  is maximum over the vineyard, having more available  $R_n$  for the soil–plant–atmosphere system and, consequently, for physical and biophysical processes required by the vineyard growth. The ratios between  $R_n$  and  $R_s^\downarrow$  were in average 0.54, 0.58, 0.57, and 0.54 for June 19–31, July, August, and September 1–18, respectively.

Based on Eqs. 5 and 6, hereafter called  $R_{n1}$  and  $R_{n2}$ , respectively, the estimated  $R_n$  values were obtained by using  $R_s^\downarrow$  measurements from the FESEBAV-2007 dataset. The same dataset was utilized to estimate the local regression coefficients  $a_1$ ,  $a_2$ ,  $b_1$ , and  $b_2$ , and the linear models obtained are shown in Table 2. Figure 5 shows the diurnal courses of the observed  $R_n$  values as well as the estimated daytime values of  $R_n$  using  $R_{n1}$  and  $R_{n2}$ , for four different days, where two of these days were under cloudless conditions (Fig. 5a, c) and the other two were cloudy (Fig. 5b, d). For these days, both  $R_{n1}$  and  $R_{n2}$  models tend to overestimate  $R_n$  slightly after 1300 hours and underestimate it slightly between 900 and 1300 hours approximately. In both cases, cloudless (day August 15, 2007: RMSE=41.93 Wm<sup>-2</sup> and MAE=37.74 Wm<sup>-2</sup>; day September 1, 2007: RMSE=36.20 Wm<sup>-2</sup> and MAE=31.94 Wm<sup>-2</sup>) and cloudy (day July 12, 2007: RMSE=

37.72 Wm<sup>-2</sup> and MAE=33.93 Wm<sup>-2</sup>; day August 23, 2007: RMSE=30.03 Wm<sup>-2</sup> and MAE=25.71 Wm<sup>-2</sup>), the estimates obtained are in good agreement with the measured values.

According to the statistical results given in Table 2, the obtained LMs showed a high accuracy in estimating  $R_{n1}$  and  $R_{n2}$ , considering that these models do not take into account the longwave component of net radiation which is obviously more significant during nighttime. At night, net radiation usually has a negative value (see Figs. 4 and 5) because there is no incoming solar radiation and the net longwave radiation is dominated by the outgoing terrestrial longwave flux. Simple regression models such as  $R_{n1}$  and  $R_{n2}$  do not contain any correction for longwave radiation nor factors affecting the longwave radiation components (Kjaersgaard et al. 2007).

During daytime, solar radiation dominates the diurnal cycle and is almost always incident to the surface, while at night, net radiation is much weaker and emerging from the surface. As a result, the surface warms up during daytime, while it cools down during evening and night hours, especially under clear sky and undisturbed weather conditions (Arya 1988). In Fig. 6, estimates of 10-min  $R_n$  values, as obtained from the models presented in Table 2, are plotted against the measured data showing high correlation coefficients ( $0.96 \leq R^2 \leq 0.97$ ), considering both the developing and the testing phases.

**Table 4** Statistical results for net radiation flux using neural networks (training/validation sets)

Model	R <sup>2</sup>	RMSE	MAE	ME
$R_{n-}$	0.92/0.92	6.23/6.54	4.59/4.76	0/0.089
$R_{n+}$	0.97/0.96	42.9/48.75	26.81/29.29	-0.33/0.26
$R_{n\pm}$	0.98/0.98	38.09/39.26	21.67/22.60	0.0209/1.41

RMSE, MAE, and ME are in units of watt per square meter

As mentioned earlier, the FESEBAV-2007 experiment was carried out over a vine crop, which somehow may be considered as sparse vegetation. During the experiment, the vineyard canopy reflectance ranges and monthly averages were respectively:  $0.15 \leq \alpha \leq 0.21$ ,  $\bar{\alpha} = 0.18$  (June);  $0.10 \leq \alpha \leq 0.22$ ,  $\bar{\alpha} = 0.17$  (July);  $0.11 \leq \alpha \leq 0.25$ ,  $\bar{\alpha} = 0.17$  (August); and  $0.11 \leq \alpha \leq 0.30$ ,  $\bar{\alpha} = 0.18$  (Septem-

ber). According to the results obtained by Alados et al. (2003), Azevedo et al. (1997); Fritschen (1967), and Kjaersgaard et al. (2007), the inclusion of the  $\alpha$  term in Eq. 6 improves only slightly the regression results as compared to Eq. 5. In this study, the statistical analysis also indicated that the inclusion of the  $\alpha$  term in Eq. 6, as compared to Eq. 5, leads to a slight improvement in  $R_n$

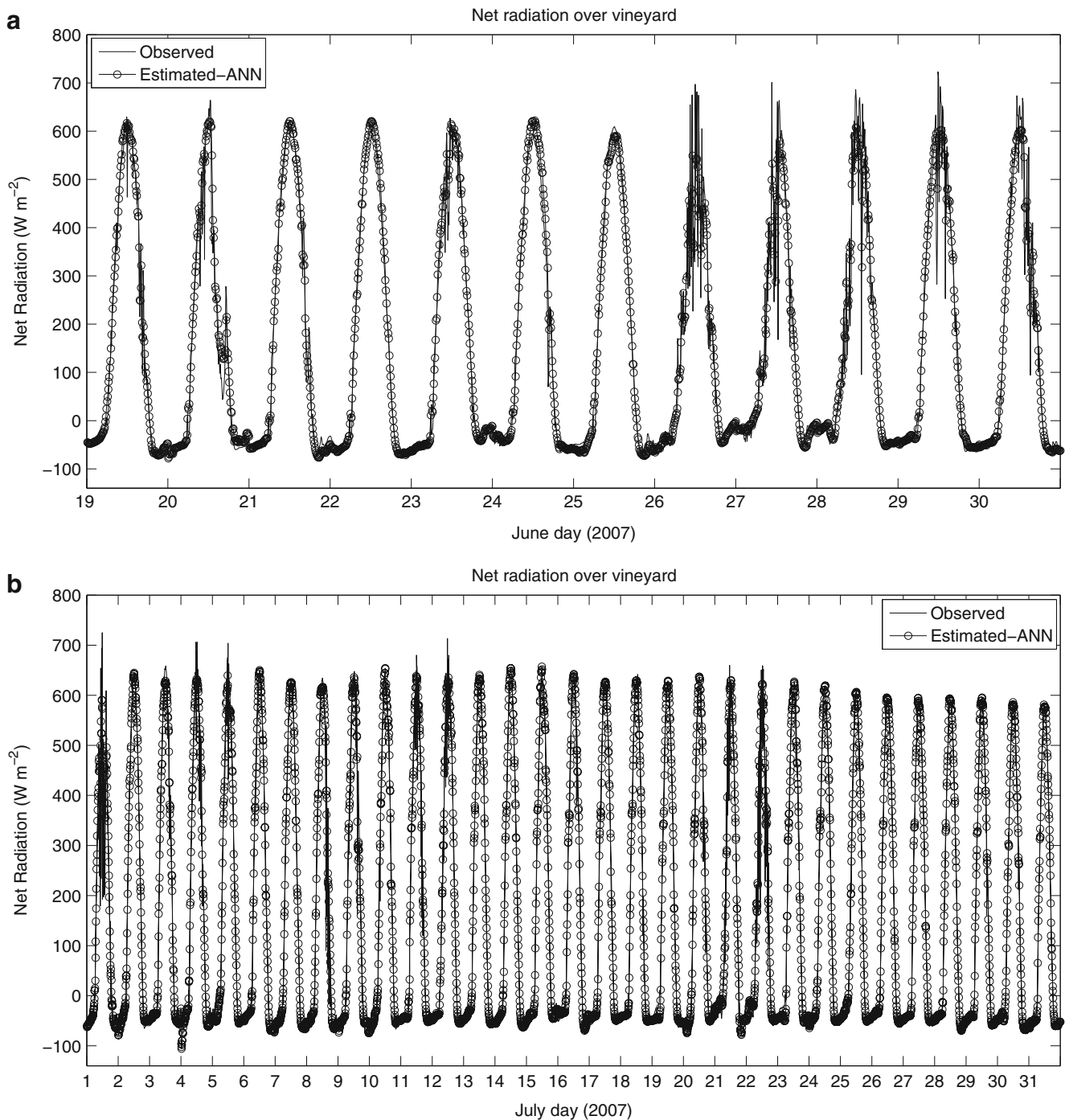


**Fig. 7** Ten-minute  $R_n$  averages measured (*lines*) and calculated by the ANN model (*dots*) for: **a** June 2007, **b** July 2007, **c** August 2007, and **d** September 2007

estimations (see  $R^2$  and RMSE on Table 2 for both models represented by these equations).

The authors mentioned above carried out their studies over irrigated field crops, European wine grape vineyard, sparse clumped shrub-land of different species, and short grass surrounded by agricultural fields, respectively. But Alados et al. (2003) reported that the inclusion of surface albedo, in the studies made by Kaminsky and Dubayah

(1997) in the boreal forest and northern prairie sites, led to a general improvement in the determination coefficients. This means that when estimating  $R_n$  at any particular place, land cover and land use need to be considered as well as the local adjustment of the model parameters.

Since  $R_s^{\downarrow}$  and  $\alpha$  are not so frequently measured in meteorological networks, the LMs presented here and those mentioned in the literature cannot be used, with reliable

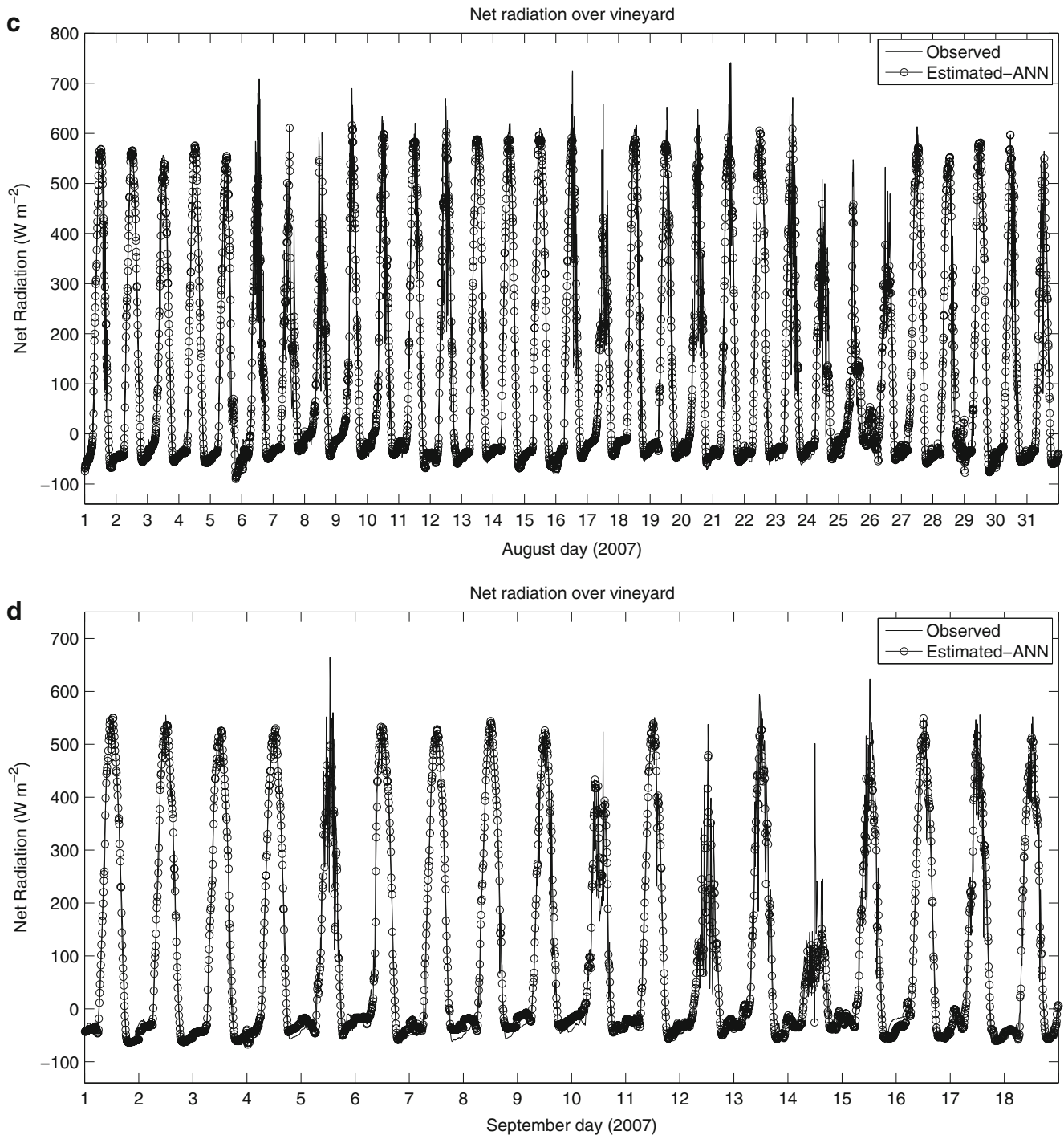
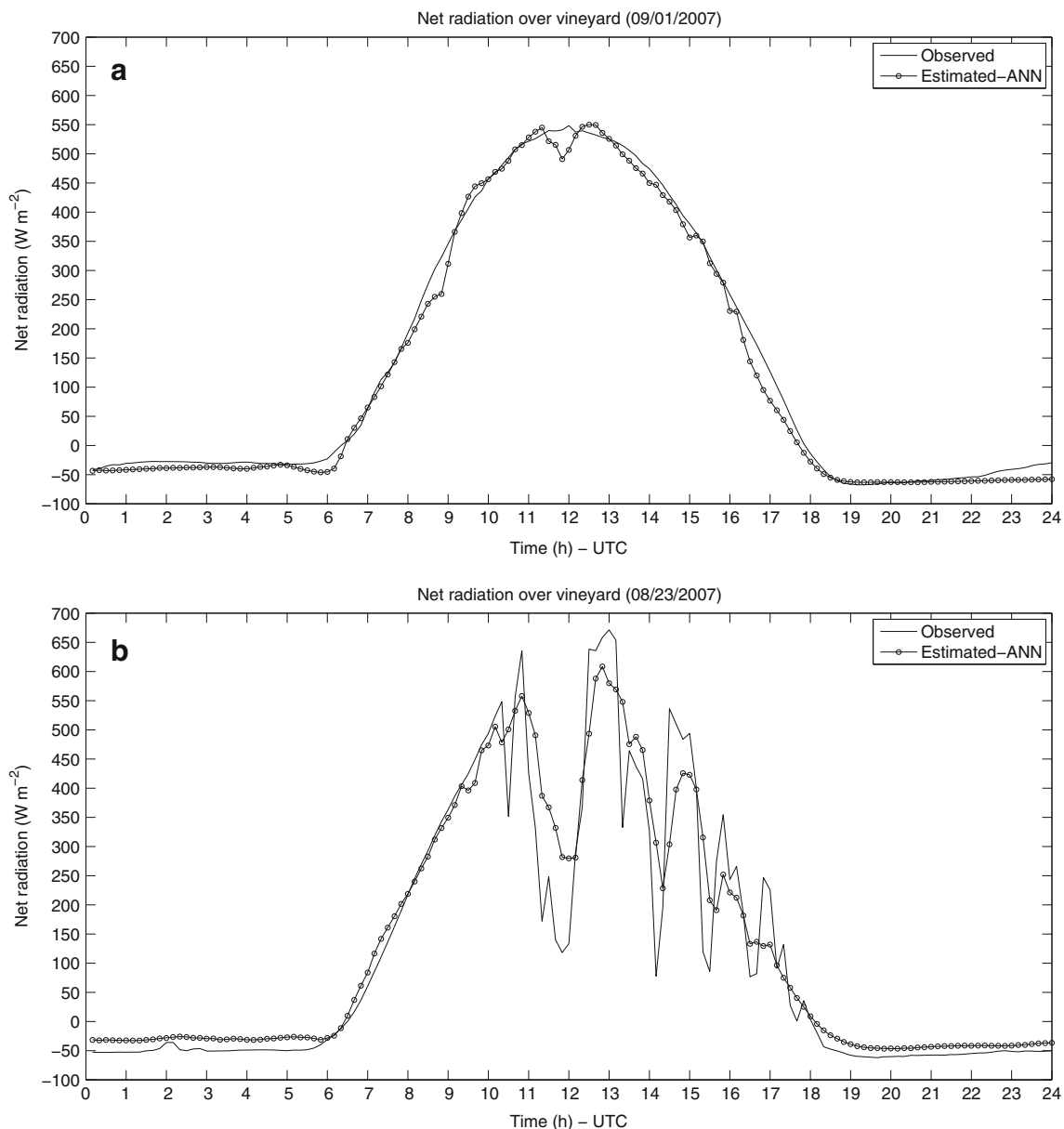


Fig. 7 (continued)

accuracy, in locations where  $R_s^\downarrow$  and  $\alpha$  are not measured. The alternative presented here to estimate  $R_n$  is modeling it using ANNs that use other meteorological parameters as input parameters. Eleven of those have been selected in this study for the estimation of  $R_n$ , namely month, day, hour, wind velocity, wind direction, air temperature, surface temperature, soil temperature, relative humidity, soil moisture, and soil heat flux (see Table 3).

ANNs of different architectures and weight initializations have been proposed and the Levenberg–Marquardt’s algorithm was selected as the procedure to adjust the neural network parameters (Luenberger and Ye 2008). This algorithm shows a better performance than other more

widely used algorithms, such as the classical *backpropagation algorithm*, for example. As far as hidden nodes are concerned, only one hidden layer was taken into consideration (the number of neurons ranged between 2 and 15). The stopping criterion was based on cross-validation (Bishop 1996; Haykin 1999). The results of this proposed ANN model for the estimation of  $R_{n\pm}$ ,  $R_{n+}$ , and  $R_{n-}$ , are shown in Table 4. As frequently indicated earlier, the calculations have been performed both for the training (they are the patterns to adjust the parameters) and for the validation (they are the patterns to avoid the overfitting) datasets. The former is used to adjust the parameters, and the latter is used to avoid overfitting.



**Fig. 8**  $R_n$  estimated by using ANN and measured  $R_n$  for clear sky conditions (days: September 1, 2007 and August 15, 2007; **a**, **c**) and for cloudy conditions (days: August 23, 2007 and July 12, 2007; **b**, **d**)

According to the results shown in Table 4, the proposed ANN model provides similar results to those from the LMs for  $R_{n1}$  and  $R_{n2}$  (see Table 2) when considering daytime values, i.e.,  $R_{n+}$ . When considering only  $R_{n-}$  (nighttime) and  $R_{n\pm}$  (full diurnal cycle), high values of  $R^2=0.92$  and  $0.98$ , respectively, for the training and the validation phases are obtained for the proposed ANN model. ANN estimated  $R_{n\pm}$  fitted well the measured data mainly over clear sky conditions (Fig. 7). The advantage of the ANN model presented here when compared to  $R_{n1}$  and  $R_{n2}$  LMs is that the ANN can also be applied to estimate  $R_n$  during the nighttime, when the sun is cutoff, and to the full diurnal

cycle of  $R_n$ , once the ANN does not use incoming solar radiation as input parameter.

Figure 8 shows the diurnal courses of  $R_{n\pm}$  estimated by the ANN model and of  $R_n$  measured at the agrometeorological station for the same 4 days presented in Fig. 5. Thus, Fig. 8a, c shows the results for the clear sky days and Fig. 8b, d for the two cloudy days. These case studies, obtained from the complete time series presented in Fig 7, show that for clear sky conditions (day August 15, 2007: RMSE=17.80  $W m^{-2}$  and MAE=13.38  $W m^{-2}$ ; day September 1, 2007: RMSE=18.33  $W m^{-2}$  and MAE=13.38  $W m^{-2}$ ) the estimates are better than for cloudy conditions

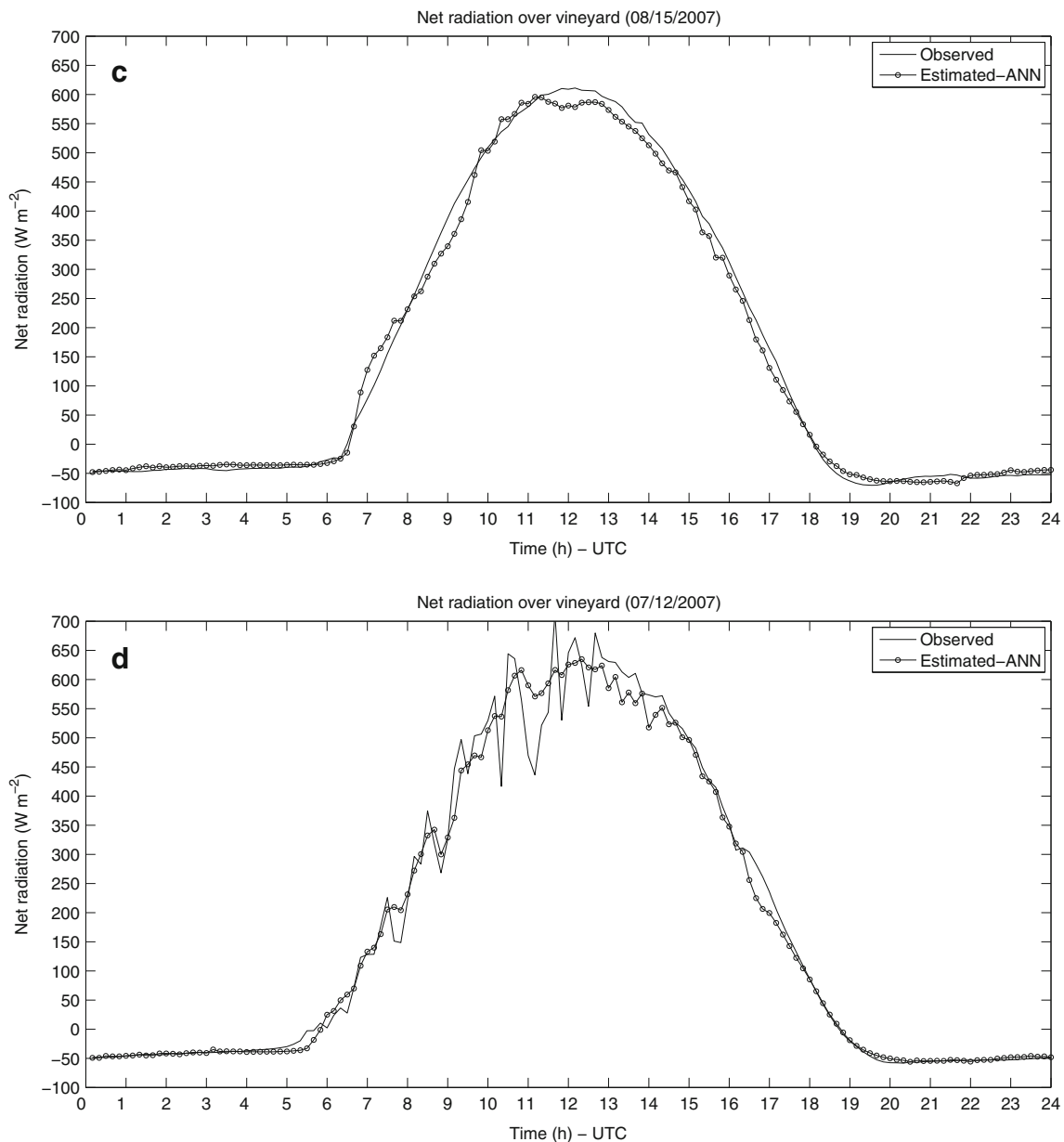


Fig. 8 (continued)



(day July 12, 2007: RMSE=31.45  $\text{Wm}^{-2}$  and MAE=18.28  $\text{Wm}^{-2}$ ; day August 23, 2007: RMSE=63.51  $\text{Wm}^{-2}$  and MAE=39.27  $\text{Wm}^{-2}$ ).

Figure 1b introduced earlier clearly showed that all radiation components are in phase under clear sky conditions and that no abrupt variation is found in the radiation components reaching the surface (Fig. 8a, c).

However, under cloudy conditions, abrupt and rapid changes appear in solar radiation reaching the surface leading to strong variations in  $R_n$  in short times (Fig. 8b, d), depending on cloud cover fraction and types, thus generating outliers in the dataset, as registered by the net radiometer (Figs. 7 and 8). These outliers are difficult to model, causing over- or underestimations of  $R_n$ , depending

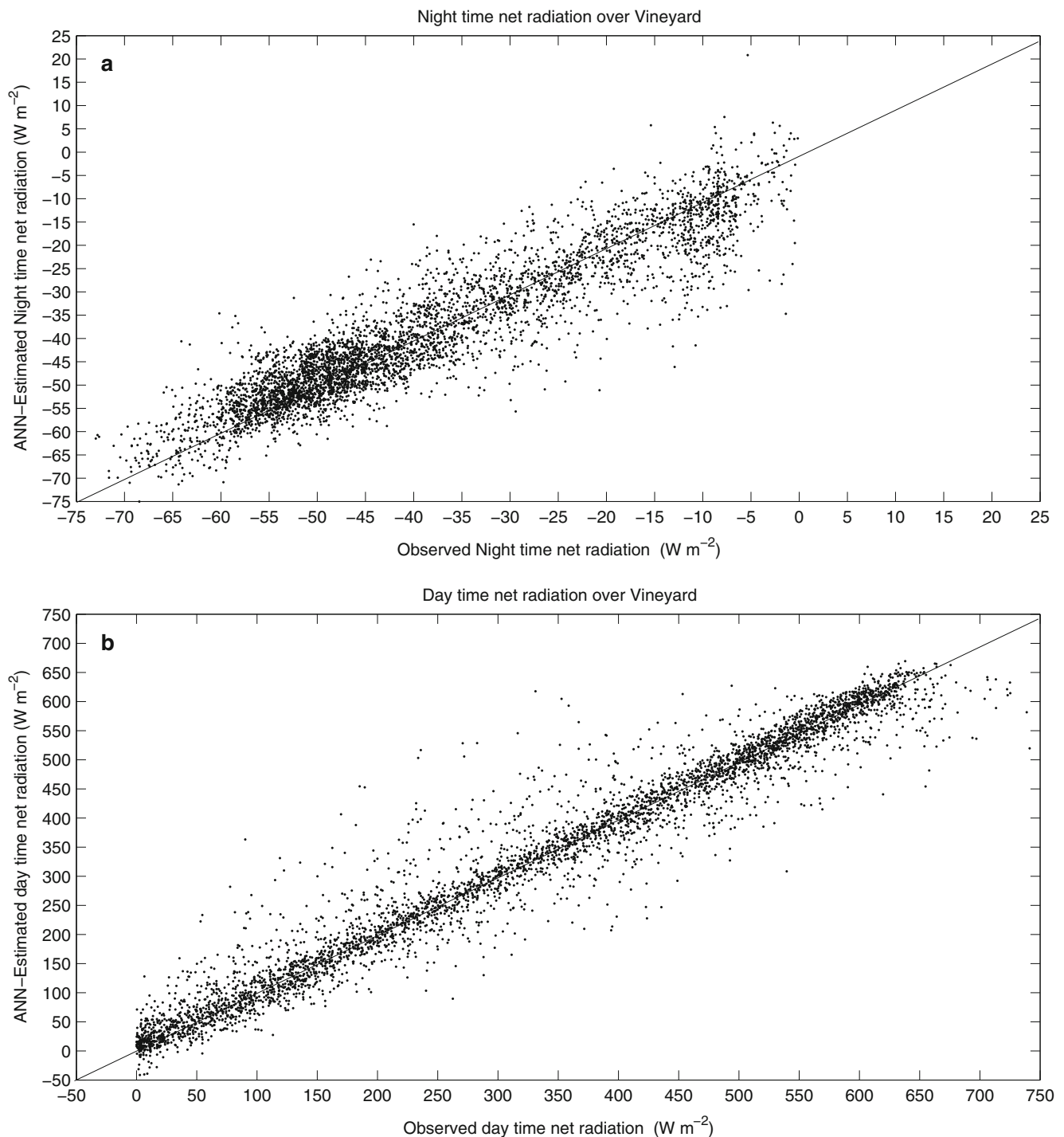


**Fig. 9** Scatter plots of net radiation (observed versus ANN estimated). **a** Nighttime, **b** daytime, and **c** complete diurnal cycle

on the period of the day, and also because the meteorological parameters used in the ANN model reflect these abrupt variations as well.

A scatter diagram between observed and estimated  $R_n$  is also shown in Fig. 9 for the three ANN models  $R_{n-}$ ,  $R_{n+}$ , and  $R_{n\pm}$ . It can be seen that these three models present low dispersion values.

Table 5 shows now the slope and intercept for LMs ( $R_{n1}$  and  $R_{n2}$ ) and ANN and the average values of measured  $R_n$ . The slopes of the lines of observed  $R_n$  versus estimated  $R_n$  are close to 1.0, varying between 0.95 and 0.98 for  $R_{n+}$  and  $R_{n\pm}$  (LMs and ANN). For  $R_{n-}$ , the slope for the ANN is 0.86. The intercepts for  $R_{n+}$  and  $R_{n\pm}$  are about 5% or less of the average measured  $R_{n+}$  and  $R_{n\pm}$  (LMs and ANN). The intercept of the ANN model for  $R_{n-}$  (nighttime) is approximately 14% of the average measured  $R_{n-}$ , and the RMSE is 16.8%. This means that the ANN improves the accuracy of the LMs considering that the latter cannot be applied for the estimation of  $R_{n-}$  or  $R_{n\pm}$ . Amarakoon and Chen (1999) considered that an intercept and RMSE of about 10% or less of the averaged measured  $R_n$  are acceptable for the different types of conditions expressed by the measured data (climate, seasons, land cover, surface moisture, soil type, etc.). In this work, we obtain similar percent values for the intercepts and RMSE when only  $R_{n+}$  values (daytime) are considered. For  $R_{n\pm}$  (diurnal cycle), the intercept and the RMSE obtained are respectively and approximately 2.7% and 21% of the averaged measured  $R_{n\pm}$ . This difference observed in the RMSE

between the acceptable values and ANN can be explained by the fact that the ANN proposed here does not use incoming solar radiation as input parameter which is directly linked to surface  $R_n$ .

As indicated earlier,  $R_s^l$  was not used as an input to the ANN, and the results clearly demonstrate that the ANN is a helpful tool to estimate  $R_n$  from meteorological data such as those mentioned in Table 3, given that parameters related to radiation fluxes are not routinely measured.

According to Irmak et al. (2003), if  $R_n$  could be predicted in an accurate manner from a minimum number of climatological data, this would be a great improvement and contribution for engineers, agronomists, climatologists, and others who routinely use regular National Weather Service climatological data such as rainfall, air temperature, atmospheric pressure, relative humidity, wind velocity, and direction. In this sense, the ANN introduced here has the ability to predict  $R_n$  using a few common meteorological parameters as input. The multilayer perceptron network uses a *learning* algorithm to determine the best network parameters to model the relationship between the input and output variables, and the adjustment between these variables is done without any assumption on previous relationships between parameters because they are actually related per se and represent sufficiently well the problem (Haykin 1999). Therefore, the methodology developed here to estimate  $R_n$  could be successfully transferred and applied to other surfaces (for example, with different land cover and land uses) and seasons.

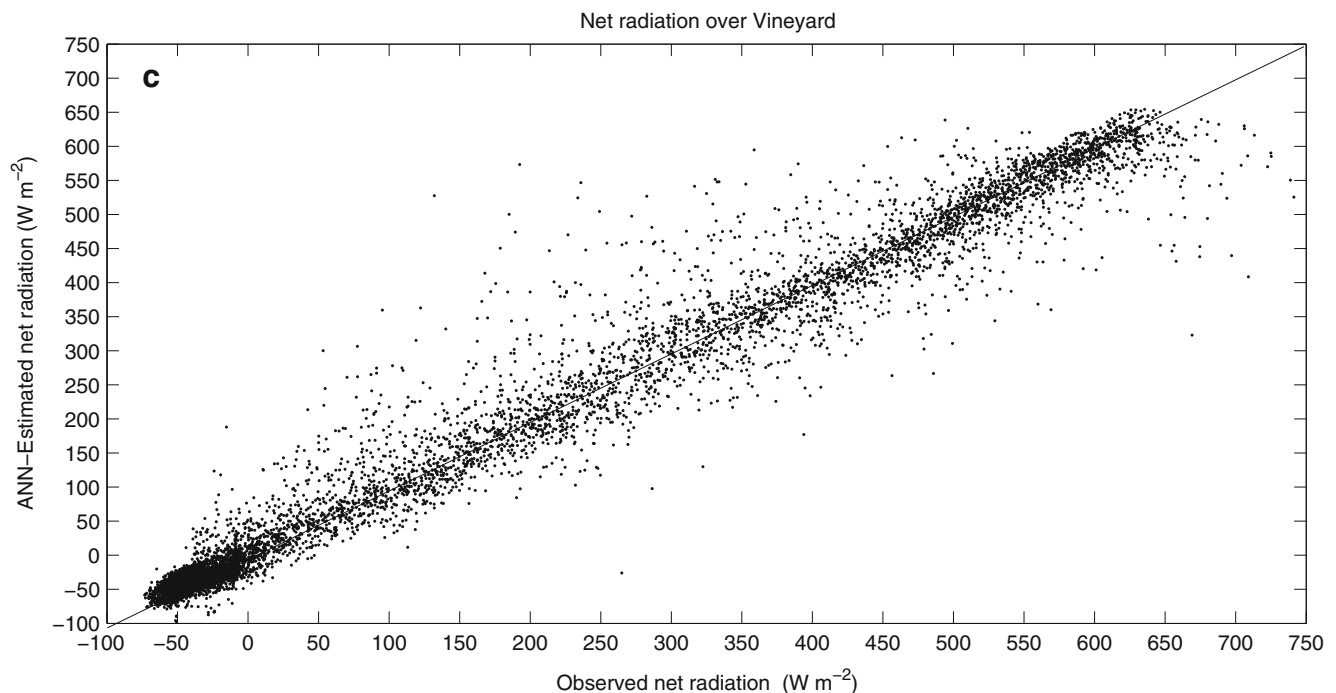


Fig. 9 (continued)



**Table 5** Linear regression ( $a$ =slope and  $b$ =intercept) between measured  $R_n$  and estimated  $R_n$  (watt per square meter) using LMs and ANN models

Model	LMs				ANN		$\overline{R_n}$
	$R_{n1}$		$R_{n2}$		$a$	$b$	
	$a$	$b$	$a$	$b$			
$R_{n+}$	0.98	5.48	0.98	4.23	0.95	16.28	330.44
$R_{n-}$	–	–	–	–	0.86	–5.50	38.94
$R_{n\pm}$	–	–	–	–	0.97	3.92	144.94

$\overline{R_n}$  is the average of measured  $R_n$ ,  $\overline{R_n}$  is given in units of watt per square meter

## 4 Conclusions

This paper presents an alternative and convenient approach to estimate surface net radiation using an artificial neural network model that uses as input variables a limited number of operational meteorological parameters currently measured in conventional agrometeorological stations. This also emphasizes the practical advantages of the method. By using the training and validation datasets, the results obtained for  $R_{n\pm}$ ,  $R_{n+}$ , and  $R_{n-}$  show the good performance of the ANN model to estimate surface  $R_n$ .

Without using  $R_s^{\downarrow}$  as input parameter, the ANN presented in this work demonstrates to be a helpful tool to estimate  $R_n$  at the surface from operational meteorological parameters such as those mentioned in Table 3, which is very useful for sites where radiation flux-related parameters are not currently measured.

Another practical advantage of the ANN in estimating  $R_n$  in comparison to other physical, empirical, or semi-empirical models, being linear or nonlinear, is that the majority of these models require other geophysical parameters such as downwelling and reflected shortwave radiation, downwelling and upwelling longwave radiation, albedo, surface temperature, air vapor pressure, fraction of cloud cover, emissivity of the surface and of the atmosphere, among others, as input to the model (Amarakoon and Chen 1999; de Jong et al. 1980; Iziomon et al. 2000; Jegede 1997; Ortega-Farias et al. 2000; Sentelhas and Gillespie 2008). Usually, these parameters are not routinely measured in agrometeorological stations, and estimations made from them may lead to increasing errors in  $R_n$  estimations.

A brief commentary should be made about the transferability of the method to other surface and seasons conditions. In spite of the neural networks being a robust tool to explore and define relationships between parameters that presumably should exist out of empirical datasets, the limitation of these models is precisely the empirical

character of the data used both for the training and for the validation phases of the procedure. In our case, the strongest variability of the data proceeds from cloudiness. Fortunately, the long dataset employed in this study has offered the possibility of seeing the behavior of the neural network under cloudy conditions of very different intensity and temporal and spatial distributions, and the model has always produced good results. Therefore, we should expect the method to be applicable to other land use conditions as well. Moreover, the study applied covering the full vineyard cycle has permitted to apply the same methodology to the very heterogeneous situations from bare soil before the beginning of the vine season to the full development of the plants that have a very heterogeneous spatial distribution, and the results are equally satisfactory.

**Acknowledgments** Antonio Geraldo Ferreira held a grant from the Programme Alβan, a European Union Programme of High Level Scholarships for Latin America, scholarship no. E05D058998BR. The field work was carried out in the framework of the projects *Calibration of SMOS MIRAS Radiometer Measurements and Generation of Maps of Salinity and of Soil Moisture Content—UVEG Part (MIDAS-4/UVEG)* and *Product Validation, Data Exploitation and Expert Center for the SMOS Mission—UVEG Part (MIDAS-5/UVEG)*, both from the Spanish Ministry for Education and Science (National Programme on Space Research), and *Remote Sensing Techniques for the Observation of Environmental Parameters in the Valencia Community Autonomous Region for 2007–2009*, from the Department for Environment, Water, Planning and Housing, General Directorate for Climate Change, Generalitat Valenciana. The authors gratefully acknowledge the owners of *El Renegado* and *Cañada Honda* vineyard fields (Caudete de las Fuentes, Valencia, Spain) where the meteorological stations are installed.

## References

- Alados I, Foyo-Moreno I, Olmo FJ, Alados-Arboledas L (2003) Relationship between net radiation and solar radiation for semi-arid shrub-land. *Agric For Meteorol* 116(3–4):221–227
- Amarakoon D, Chen A (1999) Estimating daytime net radiation using routine meteorological data in Jamaica. *Caribb J Sci* 35(1–2):132–141
- Arya SP (1988) *Introduction to micrometeorology*. Academic, London, 305 pp
- Bishop ChM (1996) *Neural networks for pattern recognition*. Clarendon, Oxford, p 482
- Azevedo PV de, Teixeira AH de C, Silva BB da, Soares JM, Saraiva FAM (1997). Avaliação da reflectância e do saldo de radiação sobre um cultivo de videira europeia. *Revista Brasileira de Agrometeorologia*, 5(1):1–7
- Carrasco M, Ortega-Farias S (2007) Evaluation of a model to simulate net radiation over a vineyard Cv Cabernet Sauvignon. *Chilean Journal of Agricultural Research* 68:156–165
- Fritschen LJ (1967) Net and solar radiation relations over irrigated field crops. *Agric Meteorol* 4:55–62
- Haykin S (1999) *Neural networks: a comprehensive foundation*. Prentice Hall, Upper Saddle River, p 842
- Irmak S, Asce M, Irmak A, Jones JW, Howell TA, Jacobs JM, Allen RG, Hooenboom G (2003) Predicting daily net radiation using

- minimum climatological data. *J Irrig Drain Eng* 129(4):256–269
- Iziomon MG, Mayer H, Matzarakis A (2000) Empirical models for estimating net radiative flux: a case study for three mid-latitude sites with orographic variability. *Astrophysics and Space Science* 273:313–330
- Jegadee OO (1997) Estimating net radiation from air temperature for diffusion modelling applications in a tropical area. *Boundary-layer Meteorology* 85:161–173
- Jegadee OO, Ogolo EO, Aregbesola TO (2006) Estimating net radiation using routine meteorological data at a tropical location in Nigeria. *International Journal of Sustainable Energy* 25(2):107–115
- de Jong R, Shaykewich CF, Reimer A (1980) The calculation of the Net radiation flux. *Archiv Für Meteorologie Geophysik Und Bioklimatologie Serie B* 28:353–363
- Kaminsky KZ, Dubayah R (1997) Estimation of surface net radiation in the boreal forest and northern prairie from shortwave flux measurements. *J Geophys Res* 102(D24):29707–29716
- Kjaersgaard JH, Cuenca RH, Plauborg FL (2007) Long-term comparisons of net radiation calculation schemes. *Boundary-Layer Meteorology* 123:417–431
- Luenberger DG, Ye Y (2008) *Linear and nonlinear programming*. International Series in Operations Research & Management Science, 3rd edition. Springer, New York, 546 pp
- Monteith JL, Unsworth MH (1990) *Principles of environmental physics*. Edward Arnold, 291 pp
- Oke TR (1987) *Boundary layer climates*, 2nd edn. Routledge, London, 435 pp
- Ortega-Farias S, Antonioletti R, Olioso A (2000) Net radiation model evaluation at an hourly time step for Mediterranean conditions. *Agronomie* 20:157–164
- Sentelhas PC, Gillespie TJ (2008) Estimating hourly net radiation for leaf wetness duration using the Penman–Monteith equation. *Theoretical and Applied Climatology* 91:205–215
- Wang K, Liang S (2008) Estimation of surface net radiation from solar shortwave radiation measurements. 978-1-4244-2808-3-IEEE-IGARSS 2008:v483–486